Chaos, Solitons and Fractals 201 (2025) 117389

Contents lists available at ScienceDirect

Chaos, Solitons and Fractals

journal homepage: www.elsevier.com/locate/chaos

Dynamics resilience of complex networks under edge-additions

Xingyue Wen [a], Jin Zhou [a,b,*], Siyang Jiang [a], Qian Zhou [a], Jun-an Lu [a]

[a] School of Mathematics and Statistics, Wuhan University, Wuhan, 430070, China
[b] Hubei Key Laboratory of Computational Science, Wuhan University, Wuhan, 430072, China

ARTICLE INFO

Keywords:
Dynamics resilience
Synchronization
Complex network

ABSTRACT

Dynamics resilience – the ability of a network to maintain stable collective dynamics under topology disturbance – is governed by the invariance of its Fiedler value. In this paper, we study dynamics resilience of complex networks under edge-additions. It is proved that networks with higher Fiedler multiplicity $r \geq 2$ exhibit remarkable dynamics resilience – adding up to $r-1$ edges will not bring about dynamics changes, as theoretically and empirically validated. To enable systematic design, we construct several network models that inherently exhibit high dynamics resilience under certain conditions.

1. Introduction

Network dynamics is one of the most pivotal areas in the field of nonlinear dynamics. In complex networks, nodes represent physical objects, with mutual physical interactions abstracted into edges between nodes. The network topology dynamically interacts with synchronization dynamics, indicating that edge-additions can substantially alter the network's nonlinear dynamical behavior. Of particular significance is Fiedler value λ_2, the second smallest eigenvalue of the Laplacian matrix associated with the network graph. Here, we refer to its algebraic multiplicity r as the Fiedler multiplicity. The Fiedler value serves as a key metric quantifying both synchronizability and diffusion efficiency [1–5]. And the greater a network's Fiedler value, the more rapidly it achieves consensus convergence [6–12]. In this work, dynamics resilience is defined as the invariance of the Fiedler value after edge-addition. Consequently, investigating the relationship between edge-addition strategies and Fiedler value's variations can uncover network's dynamics resilience – a perspective that proves vital for defending against edge-targeted attacks on network dynamics.

Based on the above definition, we aim to precisely quantify the variation in the Fiedler value after edge-additions. Existing research has focused on networks where the Fiedler value possesses a simple root [13–16]. For cases where the multiplicity of the Fiedler value exceeds 1, current literature only establishes an interlacing relationship for λ_2 after single edge-addition [17–19], while failing to provide exact quantitative bounds on its variation – thus leaving their dynamics resilience unverified. Moreover, previous studies have mentioned that network with multiple connected components, symmetric structures, or redundant topological motifs frequently exhibits multiple Fiedler value [20–24]. Although these findings highlight the critical need to investigate edge-addition effects in such multiple cases, they do not provide explicit characterization of the underlying network structures.

In light of the current research landscape, we demonstrate that networks with Fiedler multiplicity $r \geq 2$ inherently possess dynamics resilience. To be specific, we provide comprehensive proof that the network exhibits dynamics resilience provided that the Fiedler multiplicity r is at least one more than the number of added edges n. Furthermore, we extend the estimation of Fiedler value's variation when adding more than $r-1$ edges, which signifies a shift in network's dynamics. Additionally, we explore network models with high dynamics resilience under certain conditions.

* Corresponding author.
E-mail address: jzhou@whu.edu.cn (J. Zhou).

https://doi.org/10.1016/j.chaos.2025.117389
Received 13 June 2025; Received in revised form 6 September 2025; Accepted 4 October 2025
Available online 13 October 2025

2. Preliminaries

We consider an undirected, unweighted, and connected network of N diffusively coupled nonlinear oscillators, with dynamics governed by

$$\dot{\xi}_i = f\left(\xi_i\right) - c\sum_{j=1}^{N} L_{ij}\left(G\right) H\left(\xi_j\right), i = 1, 2, \ldots, N,$$

where $\xi_i \in \mathbb{R}^m$ is the state of node i. The intrinsic dynamics of an isolated node is described by a continuous nonlinear function $f \in C(\mathbb{R}^m, \mathbb{R}^m)$, while $H : \mathbb{R}^m \to \mathbb{R}^m$ represents the coupling function and c quantifies coupling strength. The network topology is characterized by its Laplacian matrix $L(G)$. It lists the N eigenvalues of $L(G)$ as $\lambda_1(G) \le \cdots \le \lambda_N(G)$ in ascending order with counting multiplicity. Of these, $\lambda_2(G)$ is the Fiedler value mentioned above, and the dynamics resilience is quantified by the invariance of the Fiedler value against edge-additions.

We now lay down the mathematical preliminaries that will underpin our analysis throughout the paper.

Lemma 1 (*Eigenvalue Interlacing Theorem [17]*). *If G^1 is obtained by adding an edge to the graph G, then the eigenvalue $\lambda_k\left(G^1\right)(1 \le k \le N-1)$ of $L\left(G^1\right)$ and the eigenvalue $\lambda_k(G)$ of $L(G)$ satisfy*

$$\lambda_k(G) \le \lambda_k\left(G^1\right) \le \lambda_{k+1}(G) \le \lambda_{k+1}\left(G^1\right).$$

Lemma 2 (*Cauchy's Interlace Theorem [25]*). *Consider a Hermitian matrix A of order m and its principal submatrix B of order $m-1$. Let the eigenvalues of A be ordered as $\lambda_1 \le \lambda_2 \le \cdots \le \lambda_{m-1} \le \lambda_m$, and the eigenvalues of B be ordered as $\mu_1 \le \mu_2 \le \cdots \le \mu_{m-1}$, then*

$$\lambda_1 \le \mu_1 \le \lambda_2 \le \mu_2 \le \cdots \le \lambda_{m-1} \le \mu_{m-1} \le \lambda_m.$$

3. Theoretical framework

This section establishes a theoretical framework to demonstrate that networks exhibiting multiple Fiedler values possess dynamics resilience. First, we construct a mathematical framework to prove that the Fiedler value with multiplicity $r\,(r \ge 2)$, remains unchanged after the network adds no more than $r-1$ edges, which reflects the dynamics resilience. Second, when the number of added edges n exceeds $r-1$, the network's dynamics resilience is compromised. And if the number of edges of the network M is large, we can estimate the variation in the Fiedler values, thereby quantifying changes in network's dynamics.

3.1. Dynamics resilience in networks with high Fiedler multiplicity under edge-additions

Theorem 1. *If the multiplicity of Laplacian eigenvalue $\lambda_k(G)$ is $r\,(r \ge 2)$, then adding $n\,(n \le r-1)$ edges arbitrarily gives graph G^n, $\lambda_k(G) = \lambda_k(G^n)$.*

Proof. Since the multiplicity of $\lambda_k(G)$ is r, which means

$$\lambda_1(G) \le \cdots \le \lambda_k(G) = \cdots = \lambda_{k+r-1}(G) \le \cdots \le \lambda_N(G).$$

According to Lemma 1, adding an arbitrary edge to G, we have $\lambda_k(G) \le \lambda_k\left(G^1\right) \le \cdots \le \lambda_{k+r-2}\left(G^1\right) \le \lambda_{k+r-1}(G)$. Therefore, we can refer that

$$\lambda_k(G) = \lambda_k\left(G^1\right) = \lambda_{k+1}\left(G^1\right) = \cdots = \lambda_{k+r-2}\left(G^1\right). \tag{1}$$

If we add one more edge to G^1, the interlacing relationships between eigenvalues are formulated by $\lambda_k\left(G^1\right) \le \lambda_k\left(G^2\right) \le \cdots \le \lambda_{k+r-3}\left(G^2\right) \le \lambda_{k+r-2}\left(G^1\right)$, we can also conclude that

$$\lambda_k\left(G^1\right) = \lambda_k\left(G^2\right) = \lambda_{k+1}\left(G^2\right) = \cdots = \lambda_{k+r-3}\left(G^2\right). \tag{2}$$

Similarly, when adding to $n\,(n \le r-1)$ edges, we have

$$\lambda_k\left(G^{n-1}\right) = \lambda_k\left(G^n\right) = \cdots = \lambda_{k+r-(n+1)}\left(G^n\right). \tag{3}$$

According to Eqs. (1), (2) and (3), we get

$$\lambda_k(G) = \lambda_k\left(G^1\right) = \lambda_k\left(G^2\right) = \cdots = \lambda_k\left(G^n\right),$$

for each $1 \le n \le r-1$. The proof is thus established. ■

According to Theorem 1, we deduce that the Fiedler value $\lambda_2(G^n)$ of the network graph G^n, which is formed by adding any $n \le r-1$ edges, remains invariant compared with the original Fiedler value $\lambda_2(G)$. This invariance demonstrates the invariance of network's dynamics, thereby confirming the network's dynamics resilience. This implies that $r-1$ serves as a critical threshold for networks with multiple Fiedler values: when the number of added edges is less than or equal to this threshold, the network demonstrates dynamics resilience. While exceeding this threshold may cause the collapse of the network's dynamics resilience.

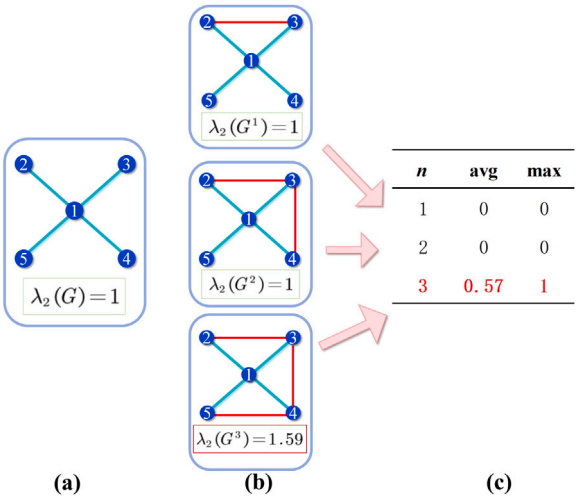

n	avg	max
1	0	0
2	0	0
3	0.57	1

Fig. 1. (a) shows the initial network with $\lambda_2 = 1$ with multiplicity 3. (b) illustrates an example of edge-additions. (c) evaluates the average and maximum Fiedler value's variations for all cases with n added edges, and the Fiedler value does not change until $n = 3$.

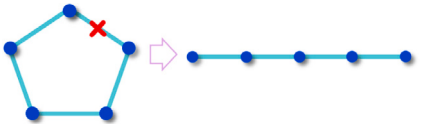

Fig. 2. Cycle network becomes a chain by deleting an edge.

We utilize a 5-node star network to validate Theorem 1. As depicted in Fig. 1(a), the Fiedler value of this star network is 1 with multiplicity 3. Fig. 1(b) illustrates a process of adding 3 edges. Observations confirm that the network maintains dynamics resilience with the successive additions of edges e_{23} and e_{34}. However, upon the subsequent addition of edge e_{45}, a significant alteration occurs in the Fiedler value, which indicates the breakdown of dynamics resilience. Moreover, we calculate the average and maximum variations of Fiedler value of all possible cases for each $n(n \leq 3)$ in Fig. 1(c), the results further substantiate the validity of Theorem 1. It demonstrates that dynamics resilience is maintained against any $n \leq 2$ added edges but collapses with a third.

Notably, our analysis of dynamics resilience applies specifically to edge-addition operations and cannot be directly applied to edge-deletion cases. For instance, for a cycle network with N nodes, the eigenvalues of $L(G)$ are $\lambda_k = 2 - 2\cos\left(\frac{2\pi(k-1)}{N}\right)$ for every $1 \leq k \leq N$. And if we delete an edge, the cycle network turns into a chain, as shown in Fig. 2 and the eigenvalue spectrum is $\lambda'_k = 4\sin^2\left(\frac{k\pi-\pi}{2N}\right)$, for each $1 \leq k \leq N$. Setting $N = 5$, $\lambda_2 = 2 - 2\cos\left(\frac{2\pi}{5}\right)$ with multiplicity 2, while $\lambda'_2 = 4\sin^2\left(\frac{\pi}{10}\right)$ with multiplicity 1. It is clear that λ_2 is not equal to λ'_2. Consequently, for networks where the Fiedler multiplicity exceeds one, the dynamics resilience does not hold under edge-deletions.

3.2. Estimation of variation in dynamics beyond $r-1$ edge-additions

For networks with dynamics resilience and when the number of added edges exceeds $r-1$, if the number of added edges n is much smaller than the total number of edges M in the network, the introduction of new edges can be treated as a small perturbation. Based on perturbation theory, we provide an estimation of the variation in the network's dynamics under such conditions by quantifying the variation in the Fiedler value.

Let the Laplacian matrix of the added edges be E. To be specific, E is formed by the Laplacian matrix of n edges separately, which is formulated as $E = E_1 + E_2 + \cdots + E_n$. For example, we consider adding edges e_{13} and e_{23} to a 4-node network, the Laplacian matrix E is

$$E = E_1 + E_2 = \begin{pmatrix} 1 & 0 & -1 & 0 \\ 0 & 0 & 0 & 0 \\ -1 & 0 & 1 & 0 \\ 0 & 0 & 0 & 0 \end{pmatrix} + \begin{pmatrix} 0 & 0 & 0 & 0 \\ 0 & 1 & -1 & 0 \\ 0 & -1 & 1 & 0 \\ 0 & 0 & 0 & 0 \end{pmatrix}.$$

Theorem 2. *When adding a set of n edges $\mathcal{E}(G)$ with $n \ll M$ to G, the variation in network's dynamics is formulated by*

$$\Delta\lambda_2 = \lambda_2(G^n) - \lambda_2(G) \approx \min_{k=1,2,\dots,r} \sum_{e_{ij}\in\mathcal{E}(G)} \left(v_{ki} - v_{kj}\right)^2, \tag{4}$$

where v_{ki} and v_{kj} denote the ith and jth components of the eigenvector v_k, and $V = (v_1, v_2, \dots, v_r)$ consists of unit orthonormal eigenvectors corresponding to the Fiedler value $\lambda_2(G)$.

Proof. Let φ_k be an eigenvector of $L(G^n)$ perturbed from v_k, with its corresponding eigenvalue adjusted to ξ_k, $k = 1, 2, \dots, r$. These quantities can be expressed as

$$\xi_k = \lambda_2(G) + \frac{1}{M}\xi_k', \tag{5}$$

and

$$\varphi_k = v_k + \frac{1}{M}v_k'. \tag{6}$$

Substituting Eq. (5) and (6) into $\xi_k\varphi_k = L(G^n)\varphi_k$, and multiplying v_k^T on the left hand side, we obtain

$$\frac{1}{M}v_k^T\xi_k' v_k + \frac{1}{M^2}v_k^T v_k'\xi_k' = \frac{1}{M}v_k^T P v_k + \frac{1}{M^2}v_k^T P v_k', \tag{7}$$

where P is represented by $P = ME$.

Ignoring $O\left(\frac{1}{M^2}\right)$ terms in Eq. (7), one gets

$$\xi_k' = \frac{v_k^T P v_k}{v_k^T v_k}. \tag{8}$$

Since v_k is a unit vector, Eq. (8) is rewritten as

$$\begin{aligned}\xi_k' &= M v_k^T\left(E_1 + \cdots + E_n\right)v_k \\ &= M\sum_{e_{ij}\in\mathcal{E}(G)}\left(v_{ki} - v_{kj}\right)^2.\end{aligned}$$

Therefore, we formulate the variation as

$$\begin{aligned}\lambda_2(G^n) - \lambda_2(G) &\approx \min_{k=1,2,\dots,r}\frac{1}{M}\xi_k' \\ &= \min_{k=1,2,\dots,r}\sum_{e_{ij}\in\mathcal{E}(G)}\left(v_{ki} - v_{kj}\right)^2.\end{aligned}$$

The proof is complete. ■

4. Network models

This section aims to identify network models that possess the advantageous property of dynamics resilience. Empirical studies reveal that networks characterized by simple Fiedler values dominate empirical observations across complex systems [26]. Conversely, networks with multiple Fiedler values often exhibit more symmetric structures and are relatively less common than those with simple Fiedler values [1]. For fundamental network models, previous studies have demonstrated that for a star network with $N \geq 3$, the Fiedler value is 1, with a multiplicity of $N-2$ [27]. Moreover, physical lattice networks often exhibit Fiedler multiplicity $r > 1$ due to their high structural symmetry. According to Theorem 1, this means that when adding edges to these lattice networks, the networks exhibit excellent dynamics resilience. This result opens up a new perspective in the dynamics of lattice networks for edge-additions and may provide critical insights for advancing physical lattice design.

In order to extend the range of network topologies exhibiting dynamics resilience, we propose two network models: a fan network characterized by a fan-like structure, and a circle-connected network centered around a circular structure. We also expand upon these two networks and identify that both the quasi-fan network and the general circle-connected network demonstrate dynamics resilience. Moreover, by incorporating a circular structure into the fan network, we find that the circle-fan network also achieves dynamics resilience.

4.1. Fan network

The fan network is derived from the star network by transforming the branch nodes into sub-networks of a similar structure. This network is dubbed a fan network due to its overall shape, which resembles a fan. The sub-network features a central node that connects to $s \geq 3$ sub-networks through p edges, and each sub-network contains m nodes, as illustrated in Fig. 3.

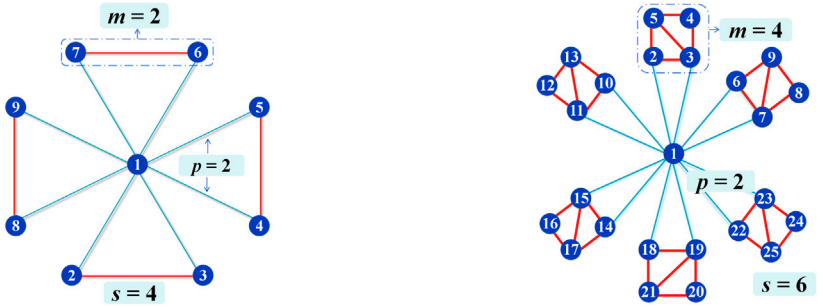

(a) $s = 4, m = 2, p = 2$ (b) $s = 6, m = 4, p = 2$

Fig. 3. Figure (a)/(b) illustrates a network with each sub-network containing $m = 2/m = 4$ nodes, featuring $s = 4/s = 6$ blades, with each blade comprising $p = 2$ edges.

The Laplacian matrix L_1 of a fan network with $ms + 1$ nodes is expressed as

$$L_1 = \begin{pmatrix} sp & -E^T & \cdots & -E^T & -E^T \\ -E^T & B + e' & \ddots & \vdots & \vdots \\ \vdots & \ddots & \ddots & 0 & 0 \\ -E^T & \cdots & 0 & B + e' & 0 \\ -E^T & \cdots & 0 & 0 & B + e' \end{pmatrix}.$$

where L_1 is a block-partitioned claw matrix. The Laplacian matrix corresponding to the fan blade is defined as B. Since the sub-network of each fan blade is connected, B is irreducible. Within B, the nodes corresponding to the first p rows and p columns are connected to the central node, and the remaining $m-p$ rows and $m-p$ columns correspond to the $m-p$ nodes that are not connected to the central node by any edge. $E = \left(\mathbf{1}^T, \mathbf{0}^T\right)^T_{1\times m}$, $\mathbf{1} = (1, \ldots, 1)^T_{1\times p}$, $\mathbf{0} = (0, \ldots, 0)^T_{1\times(m-p)}$, $e' = \begin{pmatrix} I_{p\times p} & \mathbf{0}_{p\times(m-p)} \\ \mathbf{0}_{(m-p)\times p} & \mathbf{0}_{(m-p)\times(m-p)} \end{pmatrix}_{m\times m}$, $e \in \mathbb{R}^m$ represents m-dimensional vector whose elements are all 1, $I_{p\times p}$ represents an identity matrix with p rows and p columns.

$$\begin{aligned} \det\left(L_1 - \lambda I\right) &= \begin{vmatrix} -\lambda & -E^T & \cdots & -E^T \\ -\lambda e & B + e' - \lambda I & \cdots & 0 \\ \vdots & \vdots & \ddots & \vdots \\ -\lambda e & 0 & \cdots & B + e' - \lambda I \end{vmatrix} \\ &= -\lambda \left| B + e' - \lambda I + seE^T \right| \left| B + e' - \lambda I \right|^{s-1}. \end{aligned}$$

Setting $A = B + e' + seE^T$, $C = B + e'$, $H = eE^T$, thus $A = C + sH$. $\lambda_1(A)$ and $\lambda_1(C)$ respectively formulate as

$$\lambda_1(A) = \min_{X\in\mathbb{R}^m, \|X\|=1} X^T(C + sH)X,$$

and

$$\lambda_1(C) = \min_{X\in\mathbb{R}^m, \|X\|=1} X^T C X.$$

Assuming that X_A and X_C are the eigenvectors corresponding to $\lambda_1(A)$ and $\lambda_1(C)$ respectively, which satisfy

$$X_A^T C X_A \geq X_C^T C X_C, \tag{9}$$

$$X_A^T sH X_A \geq \lambda_1(sH) = 0. \tag{10}$$

By adding the left-hand sides and the right-hand sides of inequalities Eq. (9) and Eq. (10) respectively, we get

$$\lambda_1(A) \geq \lambda_1(C).$$

Thus, we conclude that

$$\lambda_2\left(L_1\right) = \lambda_1(C) = \lambda_1\left(B + e'\right),$$

and it is easy to see that the multiplicity of the eigenvalue $\lambda_2\left(L_1\right)$ is $s - 1$.

Consequently, according to Theorem 1, the network exhibits dynamics resilience by the arbitrary addition of $n \leq s - 2$ edges, which means that $s - 2$ is the threshold for dynamics transition of fan networks.

To investigate the relationship between the Fiedler value of the fan network and the parameters m, s, and p, we assume that each sub-network is in a fully connected state. We then explore the relationship between the Fiedler value $\lambda_2(L_1)$ and these parameters,

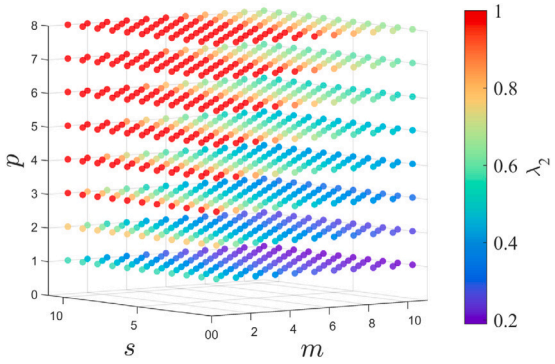

Fig. 4. Heatmap of the fan network. $\lambda_2(L_1)$ increases with increasing edges p to sub-networks and decreasing nodes m per sub-network, while it is independent of s.

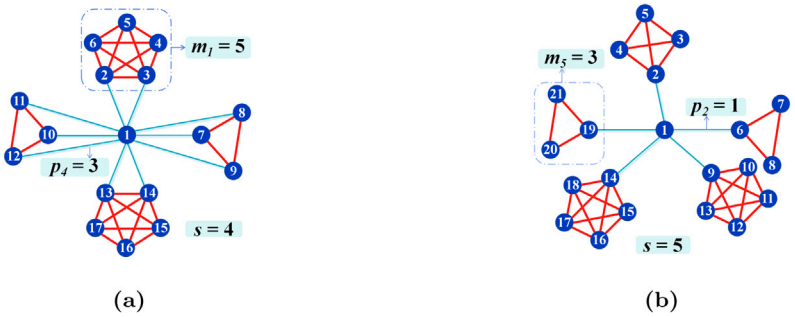

Fig. 5. The network consists of 4 blades in Fig. (a) and 5 blades in Fig. (b), with varying connections to sub-networks of 3, 4, and 5 nodes through 1 to 3 edges.

and present the resulting heatmap in Fig. 4. From Fig. 4 we can clearly see that, the Fiedler value of a network is enhanced when there are more edges p connecting the central node to the sub-networks and fewer nodes m within each sub-network with a fixed s. Moreover, this network's Fiedler value is independent of the number of sub-networks s.

4.2. Quasi-fan network

A quasi-fan network is an evolution of the fan network, characterized by variations in the structure of its blades and the connections to the central node, as shown in Fig. 5. Unlike the fan network, the quasi-fan network permits each blade to have a distinct way of connection, and the manner in which each blade connects to the central node can also vary. Let s be the number of blades in the network. For the ith blade, m_i signifies the number of nodes within the blade, p_i represents the number of nodes that are directly connected to the central node.

The Laplacian matrix of quasi-fan network L_1' is

$$L_1' = \begin{pmatrix} p_1 + p_2 + \cdots + p_s & -E_1^T & \cdots & -E_s^T \\ -E_1 & B_1 + e_1' & \cdots & 0 \\ \vdots & \vdots & \ddots & \vdots \\ -E_s & 0 & \cdots & B_s + e_s' \end{pmatrix}, \tag{11}$$

where L_1' is a block-partitioned claw matrix. The Laplacian matrix for the ith fan blade is denoted as B_i, which is recognized as an irreducible matrix. The variable m_i denotes the number of nodes within the ith sub-network. Within the matrix B_i, the nodes corresponding to the first p_i rows and p_i columns are connected to the central node in the quasi-fan network. The remaining $m_i - p_i$ rows and $m_i - p_i$ columns represent the nodes that are not linked to the central node. The matrix E_i is defined as $\left(\mathbf{1}^T, \mathbf{0}^T\right)^T_{1\times m_i}$, where $\mathbf{1} = (1, \ldots, 1)^T_{1\times p_i}$ and $\mathbf{0} = (0, \ldots, 0)^T_{1\times(m_i-p_i)}$. Additionally, e_i' is given by the matrix $\begin{pmatrix} I_{p_i\times p_i} & \mathbf{0}_{p_i\times(m_i-p_i)} \\ \mathbf{0}_{(m_i-p_i)\times p_i} & \mathbf{0}_{(m_i-p_i)\times(m_i-p_i)} \end{pmatrix}_{m_i\times m_i}$, with $I_{p_i\times p_i}$ being the $p_i \times p_i$ identity matrix.

By deleting the first row and column from Eq. (11), we obtain the principal submatrix A_1. Let the eigenvalues of A_1 be sorted in ascending order as $\mu_1 \le \mu_2 \le \cdots \le \mu_{m_1+m_2+\cdots+m_s}$. By Lemma 2, we have

$$0 = \lambda_1\left(L_1'\right) \le \mu_1 \le \lambda_2\left(L_1'\right) \le \cdots \le \lambda_{(m_1+m_2+\cdots+m_s)}\left(L_1'\right). \tag{12}$$

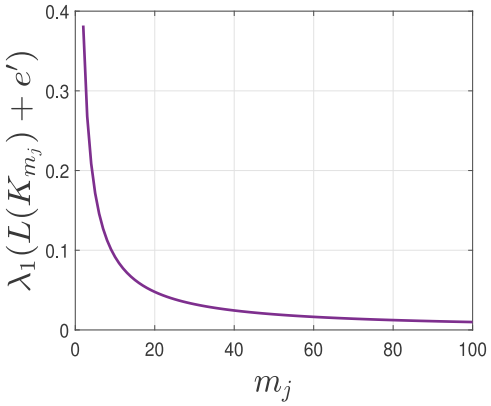

Fig. 6. Relationship between $\lambda_1\left(L\left(K_{m_j}\right)+e'\right)$ and m_j.

Since $\left|\left\{i\in\mathcal{I}:\lambda_1\left(B_i+e_i'\right)=\min_{j\in\mathcal{I}}\lambda_1\left(B_j+e_j'\right)\right\}\right|=a$ and $\mu_1=\min_{j\in\mathcal{I}}\lambda_1\left(B_j+e_j'\right)$, we have

$$\mu_1=\mu_2=\cdots=\mu_a. \tag{13}$$

Combining Eq. (12) and (13), we obtain $\lambda_2\left(L_1'\right)=\lambda_3\left(L_1'\right)=\cdots=\lambda_a\left(L_1'\right)$, which indicates that the multiplicity of $\lambda_2\left(L_1'\right)$ is at least $a-1$. Similar to the derivation process of the fan network, we find

$$\lambda_2\left(L_1'\right)=\min_{j\in\mathcal{I}}\lambda_1\left(B_j+e_j'\right).$$

Therefore, for a quasi-fan network, if $\left|\left\{i\in\mathcal{I}:\lambda_1\left(B_i+e_i'\right)=\min_{j\in\mathcal{I}}\lambda_1\left(B_j+e_j'\right)\right\}\right|=a(a\geq 3)$, then $\lambda_2\left(L_1'\right)=\min_{j\in\mathcal{I}}\lambda_1\left(B_j+e_j'\right)$ with the multiplicity at least $a-1$. Among them, the cardinality $|\cdot|$ is used to represent the number of elements in the set, $\mathcal{I}$ represents the set of sub-networks serial numbers $\{1,2,\ldots,s\}$.

Notably, for quasi-fan networks, the determination of both Fiedler multiplicity and dynamics resilience can be significantly simplified by examining the structure of the sub-networks and their connection to the central node. This finding substantially diminishes the computational complexity involved in the analysis of the entire network.

When all sub-networks are fully connected networks with m_j nodes and each sub-network has only one edge connected to the central node, we have

$$B_j+e_j'=L\left(K_{m_j}\right)+e'=\begin{pmatrix} m_j & -1 & -1 & \cdots & -1\\ -1 & m_j-1 & -1 & \cdots & -1\\ -1 & -1 & m_j-1 & \cdots & -1\\ \vdots & \vdots & \vdots & \ddots & \vdots\\ -1 & -1 & -1 & \cdots & m_j-1 \end{pmatrix},$$

where K_{m_j} is fully connected with m_j nodes in L_1'.

Since the relationship between $\lambda_1\left(L\left(K_{m_j}\right)+e'\right)$ and the number of nodes m_j in each sub-network cannot be explicitly formulated, it is essential to employ numerical computation methods to investigate this issue in detail. Fig. 6 illustrates a monotonically decreasing relationship between the number of sub-network nodes and $\lambda_1\left(L\left(K_{m_j}\right)+e'\right)$.

4.3. Circle-connected network

A circle-connected network has a central circle surrounded by identically structured sub-networks that the networking topology exhibits uniform connectivity, and each node on the central circle also serves as a node within one of the sub-networks, as presented in Fig. 7. The network includes a central circle of order $s\geq 3$ and s identical sub-networks. Within each sub-network, there are m nodes, and each sub-network is connected.

The Laplacian matrix of a circle-connected network with ms nodes is expressed as

$$L_2=\begin{pmatrix} B+Y_0 & -X_0 & & & -X_0\\ -X_0 & B+Y_0 & -X_0 & & \\ & -X_0 & B+Y_0 & & \\ & & & \ddots & -X_0\\ -X_0 & & & -X_0 & B+Y_0 \end{pmatrix},$$

where B is the Laplacian matrix corresponding to the sub-network. X_0 is a matrix with 1 in the first row and first column, while zeros elsewhere, and $Y_0=2X_0$.

Fig. 7. Figure (a)/(b) illustrates a network with each sub-network containing $m = 5/m = 4$ nodes, arranged around a central circle of order 3 or 6.

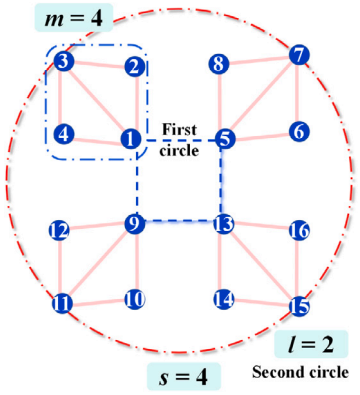

Fig. 8. A general circle-connected network with $s = 4$ sub-networks, each containing $m = 4$ nodes, linked via 2 circles.

Let h be a matrix with ones on the first superdiagonal and at the bottom left corner. Thus, $2I - h - h^{s-1}$ is a cyclic tridiagonal matrix, and L_2 is denoted by

$$L_2 = I_s \otimes (B + Y_0) - h \otimes X_0 - h^{s-1} \otimes X_0.$$

The eigenvalue of h is the root of $\lambda^s - 1 = 0$, yields $\omega_k = \cos\frac{2k\pi}{s} + i\sin\frac{2k\pi}{s}, 1 \le k \le s$. It is evident that the reciprocal of ω_k is its conjugate, thus $\omega_k + \omega_k^{s-1} = \omega_k + \frac{1}{\omega_k} = \omega_k + \overline{\omega_k} = 2\cos\frac{2k\pi}{s}$. Therefore, we have

$$\begin{aligned} |\lambda I - L_2| &= \prod_{k=1}^{s} \left|\lambda I - (B + Y_0) + \omega_k X_0 + \omega_k^{s-1} X_0\right| \\ &= \prod_{k=1}^{s} \left|\lambda I - B - 4\sin^2\frac{k\pi}{s} X_0\right|. \end{aligned}$$

Since the matrix $4\sin^2\frac{k\pi}{s}X_0$ has eigenvalues with only one eigenvalue of 1, all other eigenvalues are 0. Since B is a symmetric matrix, $\lambda_1(L_2) = \lambda_1(B) = 0$. According to Courant–Weyl inequalities [28], we deduce that $\lambda_2(L_2) = \lambda_1\left(B + 4\sin^2\frac{\pi}{s}X_0\right) = \lambda_1\left(B + 4\sin^2\frac{(s-1)\pi}{s}X_0\right)$ and its multiplicity is always 2. Thus, dynamics resilience is preserved under single edge-addition.

When the sub-network reduces to a single node, the circle-connected network simplifies to a cycle network. And the characteristic polynomial of L_2 is $\prod_{k=1}^{s}\left|\lambda - 4\sin^2\frac{k\pi-\pi}{s}\right|$, which is similar to the results previously mentioned.

4.4. General circle-connected network

Extending the concept of a circle-connected network to a more general scenario, if l $(2 \le l \le m)$ s-order circles are employed to connect identical sub-networks in the same manner, as shown in Fig. 8.

Denote

$$X_0' = \begin{pmatrix} 1 & 0 & & \\ 0 & 1 & & \\ & & \ddots & \\ & & & 0 \end{pmatrix}, Y_0' = 2X_0',$$

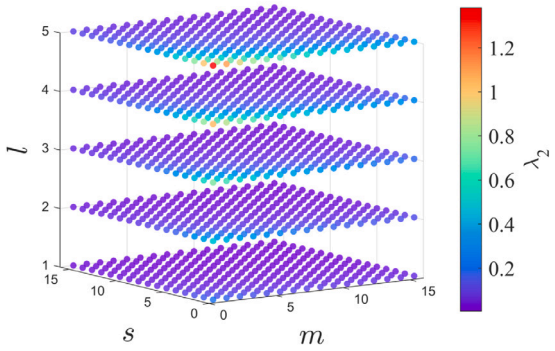

Fig. 9. Heatmap shows how $\lambda_2(L_2')$ for a general circle-connected network varies with m, s, and l. $\lambda_2(L_2')$ decreases with increasing s or m when l is constant, and with increasing m or decreasing l when s is fixed. It also drops as s increases or l decreases with m held constant.

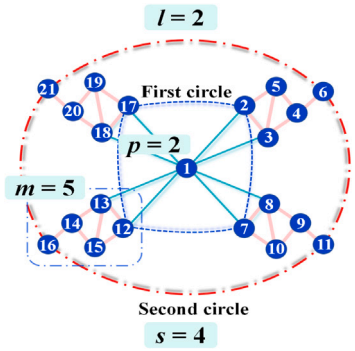

Fig. 10. In a circle-fan network, a central node is connected to $s = 4$ sub-networks, each with $m = 5$ nodes via $p = 2$ edges per blade, and these sub-networks are interconnected through $l = 2$ circles.

where the first l rows and l columns of X_0' with the elements on the main diagonal being 1 and the rest being 0. Correspondingly, the Laplacian matrix L_2' of the general circle-connected network is

$$L_2' = \begin{pmatrix} B+Y_0' & -X_0' & & & -X_0' \\ -X_0' & B+Y_0' & -X_0' & & \\ & -X_0' & B+Y_0' & & \\ & & & \ddots & -X_0' \\ -X_0' & & & -X_0' & B+Y_0' \end{pmatrix}.$$

Similar to the above derivation, we refer that if the Fiedler value of L_2' has the multiplicity at least 2,

$$\lambda_2(B) \geq \lambda_1\left(B + 4\sin^2\frac{k\pi}{s}X_0'\right).$$

It is observed that the number l of central circles connecting to sub-networks in the same manner identically determines whether the Fiedler value is multiple or not, which consequently governs whether the network can exhibit dynamics resilience under edge-additions.

To investigate how network's dynamics are influenced by m, s, and l in fully connected sub-networks, we examine the relationship between $\lambda_2(L_2')$ and these variables. As shown in Fig. 9, if l holds constant, $\lambda_2(L_2')$ decreases with an increase in the number of sub-networks s and the number of nodes m per sub-network. Moreover, with a constant s, $\lambda_2(L_2')$ decreases as both l and m increase. Notably, fixing m and reducing s while increasing l significantly enhances the network's dynamics.

4.5. Circle-fan network

After adding l circles to the fan network in the same way, the circle-fan network is shown in Fig. 10. Define L_3 as the Laplacian

(a) (b)

Fig. 11. Wheel network with $s+1$ nodes.

matrix of the circle-fan network, and it is represented as

$$L_3 = \begin{pmatrix} sp & -E^T & -E^T & \cdots & -E^T \\ -E & B+e'+Y_0' & -X_0' & \cdots & -X_0' \\ -E & -X_0' & B+e'+Y_0' & \cdots & 0 \\ \vdots & \vdots & \vdots & \ddots & \vdots \\ -E & -X_0' & 0 & \cdots & B+e'+Y_0' \end{pmatrix}.$$

In line with the derivation in the preceding models, if $\lambda_1\left(B+e'+seE^T\right) \geq \lambda_1\left(B+e'+4\sin^2\frac{k\pi}{s}X_0'\right)$, the circle-fan network displays dynamics resilience.

When the sub-network is a node, the fan network transitions into a wheel network (see Fig. 11). It is easy that the Fiedler value of a wheel network with $s+1$ nodes is $1+4\sin^2\frac{\pi}{N}$ and has multiplicity 2. This implies the network exhibits its dynamics resilience under arbitrary addition of any single edge.

5. Experiments and results

To validate the impact of edge-additions on networks with high dynamics resilience and the threshold $r-1$, we added edges to both the physical lattice networks and the aforementioned network models. We quantitatively compare the actual variations in Fiedler values against their theoretical variations (as obtained by Theorems 1 and 2), thereby verifying the feasibility conditions of the proposed theory.

We first consider three representative physical lattice networks with Fiedler multiplicity $r=2$: graphene lattice (15 edges), ruby lattice (132 edges), and kagome lattice (18 edges). We conducted 100 randomized edge-addition experiments on the networks to compare theoretical and actual Fiedler value's variations. As depicted in Fig. 12, the network exhibits dynamics resilience when adding $r-1=1$ edge. When more than $r-1$ edges are added, the ruby lattice exhibits significantly smaller deviations between actual and theoretical Fiedler value's variations compared to other physical lattice networks, suggesting higher estimation accuracy. This observed phenomenon correlates strongly with the ruby lattice's characteristically higher edge count M. For sparsely connected lattices (graphene and kagome lattices), the Fiedler value estimation becomes biased when the number of added edges n exceeds 2.

Furthermore, we investigate the constructed fan networks with increased edge count M, aiming to broaden the analytical perspective and validate the reliability of our theoretical framework.

We construct fan networks with edge counts $M=40,150,230$, and 700, whose corresponding Fiedler multiplicities are 4, 9, 9, and 19, respectively. When the edge count M is small, the variations between actual and theoretical values remain significant as shown in Fig. 13. These variations decrease dramatically to $O(10^{-4})$ as M increases, confirming the method's critical dependence on M and quantitatively satisfying $n \ll M$ at $M>500$ to bound $\Delta\lambda_2$'s deviation. Moreover, we verify that increasing the number of fan blades s induces a proportional growth in structurally similar sub-networks, which in turn enhances network symmetry, thereby leading to higher Fiedler multiplicity r as well as higher threshold $s-2$ for dynamics transition.

To systematically investigate the relationship between network edge count M and the precision of Fiedler value estimation, we formally define the relative error:

$$\delta_n = \frac{\left|\Delta\lambda_2^{actual} - \Delta\lambda_2^{theoretical}\right|}{\Delta\lambda_2^{actual}}, \tag{14}$$

where $\Delta\lambda_2^{actual}$ indicates the actual change in Fiedler value after adding n edges. And $\Delta\lambda_2^{theoretical} = \min_{k=1,2,\ldots,r}\sum_{e_{ij}\in\mathcal{E}(G)}\left(v_{ki}-v_{kj}\right)^2$, which is the theoretical estimation proposed in Theorem 1.

Since the threshold for dynamics transition of the fan network is $s-2$ as described in the construction process of the model above. When the number of nodes of the fan blades $m=5$ and the number of edges connecting the center node and the fan blades $p=2$ are fixed, the number of edges added to the network is the same for every 1 unit increase in the number of fan blades s. Therefore, the discussion of the increase in the number of edges M can be transformed into a discussion of the increase in s, and further a quantitative relationship can be established with the Fiedler multiplicity r. Fig. 14 demonstrates that the estimation accuracy of the Fiedler variation shows significant improvement with increasing values of parameter s.

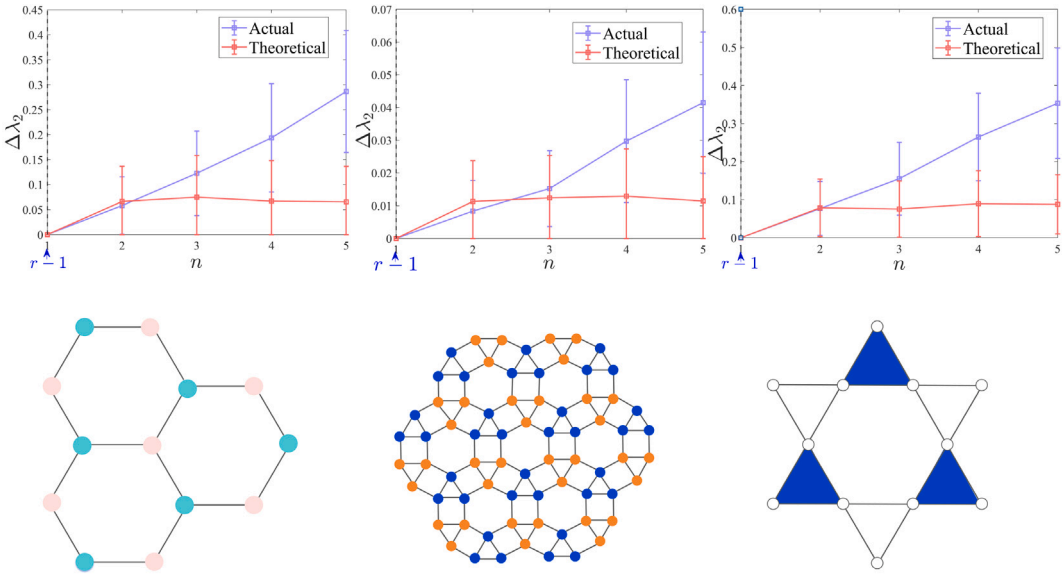

(a)Graphene lattice (b)Ruby lattice (c)Kagome lattice

Fig. 12. Comparative analysis of theoretical versus actual Fiedler values for three physical lattice networks (graphene, kagome [29], and ruby lattices [30]) with their corresponding network graphs. The ruby lattice, possessing the highest edge count M, demonstrates exceptional agreement between theoretical and actual Fiedler values, while the remaining two lattice networks achieve inferior estimation precision.

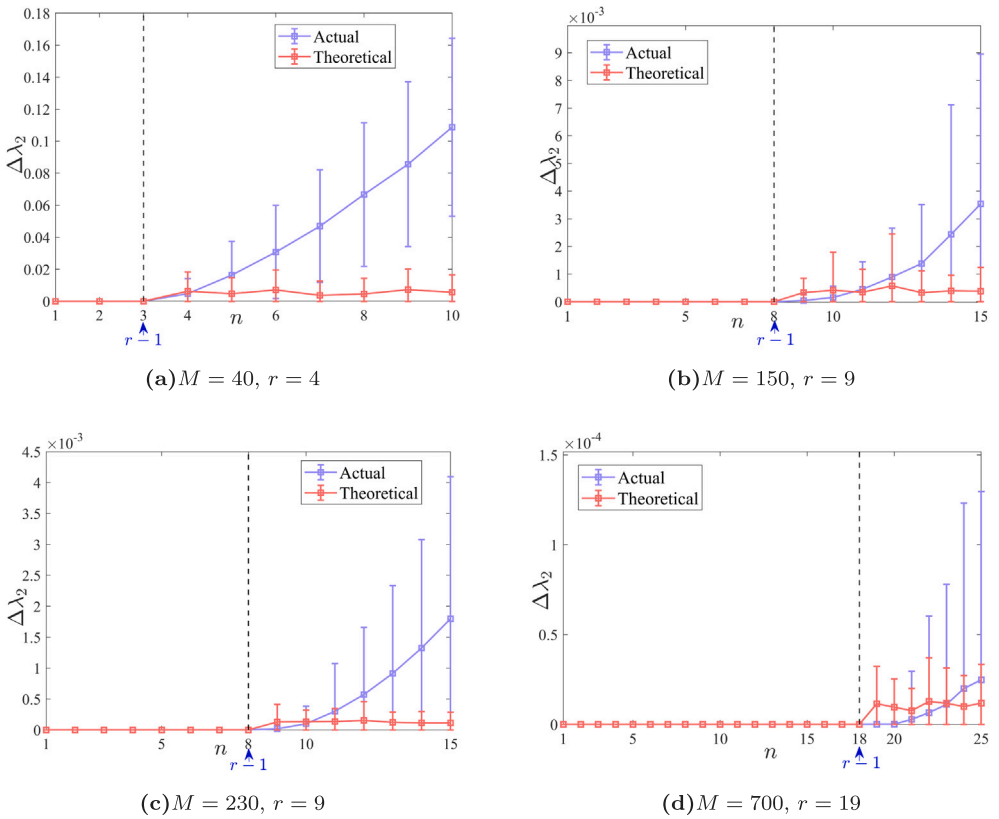

(a)$M = 40,\ r = 4$ (b)$M = 150,\ r = 9$

(c)$M = 230,\ r = 9$ (d)$M = 700,\ r = 19$

Fig. 13. Using four representative fan networks, it shows Fiedler value estimation errors decay from $O(10^{-1})$ to $O(10^{-4})$ as edge count M increases, revealing M-dependent accuracy.

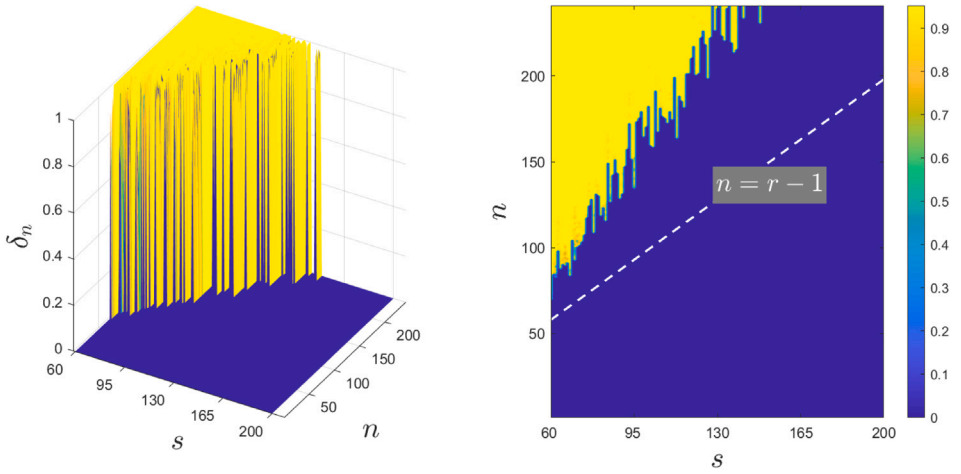

Fig. 14. The relative error δ_n (defined in Eq. (14)) of adding n edges decreases as the number of blades s increases with other parameters fixed in fan networks, demonstrating enhanced estimation accuracy with greater edge count M.

6. Conclusion

We have investigated that networks with Fiedler multiplicity $r \geq 2$ exhibit dynamics resilience when $n \leq r - 1$ edges are added through mathematical analysis, which has been verified in some network models, *i.e.*, fan network, circle-connected network, quasi-fan network, general circle-connected network and circle-fan network. This implies that the network's structural integrity and its ability to maintain dynamics or resist disruptions are enhanced by the presence of this high Fiedler multiplicity. The results have provided a theoretical foundation for understanding dynamics in real networks exhibiting dynamics resilience, such as lattice materials. Furthermore, our findings may extend to social network dynamics, biological networks and communication infrastructures [31–34].

CRediT authorship contribution statement

Xingyue Wen: Writing – original draft, Visualization, Validation, Software, Methodology, Investigation, Formal analysis. **Jin Zhou:** Writing – review & editing, Supervision, Methodology, Funding acquisition, Conceptualization. **Siyang Jiang:** Writing – review & editing, Methodology. **Qian Zhou:** Methodology. **Jun-an Lu:** Writing – review & editing, Supervision, Methodology, Funding acquisition, Conceptualization.

Declaration of competing interest

The authors declare that they have no known competing financial interests or personal relationships that could have appeared to influence the work reported in this paper.

Acknowledgments

This work is supported by the National Natural Science Foundation of China under Grant 62573330, Grant 62173254, Grant 62176099, and the Fundamental Research Funds for the Central Universities under Grant 2042025kf0088.

Data availability

No data was used for the research described in the article.

References

[1] Fiedler M. Algebraic connectivity of graphs. Czechoslovak Math J 1973;23(2):298–305.
[2] Gancio J, Rubido N. Critical parameters of the synchronisation's stability for coupled maps in regular graphs. Chaos Solitons Fractals 2022;158:112001.
[3] Carballosa A, Crego Á, Muñuzuri AP. Quantifying the potentiality for polarization in opinion networks. Chaos, Solitons Fractals 2023;173:113697.
[4] Gao S, Zhang S, Chen X. Effects of changing the weights of arcs on the consensus convergence rate of a leader–follower multi-agent system. Chaos Solitons Fractals 2023;172:113590.
[5] Hwang DU, Chavez M, Amann A, Boccaletti S. Synchronization in complex networks with age ordering. Phys Rev Lett 2005;94(13):138701.

[6] Peng XJ, He Y, Li H, Tian S. Consensus control and optimization of time-delayed multiagent systems: Analysis on different order-reduction methods. IEEE Trans Syst Man Cybern: Syst 2025;55(1):780–91.
[7] Peng XJ, He Y, Liu Z, You L, Li H. Time-varying formation H_∞ tracking control and optimization for delayed multi-agent systems with exogenous disturbances. IEEE Trans Autom Sci Eng 2025;22:5637–47.
[8] Wang X, Chen G. Synchronization in small-world dynamical networks. Int J Bifurc Chaos 2002;12(01):187–92.
[9] Gomez S, Diaz-Guilera A, Gómez-Gardeñes J, Perez-Vicente CJ, Moreno Y, Arenas A. Diffusion dynamics on multiplex networks. Phys Rev Lett 2013;110(2):028701.
[10] Yu C, Xiao W. Synchronizability and synchronization rate of AC microgrids: A topological perspective. IEEE Trans Netw Sci Eng 2023;11(2):1424–41.
[11] Kempton L, Herrmann G, Di Bernardo M. Self-organization of weighted networks for optimal synchronizability. IEEE Trans Control Netw Syst 2017;5(4):1541–50.
[12] McLoughlin C, Lowery M. Impact of network topology on neural synchrony in a model of the subthalamic nucleus-globus pallidus circuit. IEEE Trans Neural Syst Rehabil Eng 2023;32:282–92.
[13] Yang Y, Tu L, Guo T, Chen J. Spectral properties of supra-Laplacian for partially interdependent networks. Appl Math Comput 2020;365:124740.
[14] Jiang S, Zhou J, Small M, Lu JA, Zhang Y. Searching for key cycles in a complex network. Phys Rev Lett 2023;130(18):187402.
[15] Zhou J, Zhang Y, Lu JA, Chen G. Introducing a new edge centrality measure: The connectivity rank index. IEEE Trans Syst Man Cybern: Syst 2024;54(5):2757–64.
[16] Jiang S, Lu JA, Zhou J, Dai Q. Fiedler value: The cumulated dynamical contribution value of all edges in a complex network. Phys Rev E 2024;109(5):054301.
[17] Mohar B, Alavi Y, Chartr G, Oellermann O. The Laplacian spectrum of graphs. In: Graph theory, combinatorics, and applications. New York: Wiley; 1991, p. 871–98.
[18] Van Den Heuvel J. Hamilton cycles and eigenvalues of graphs. Linear Algebra Appl 1995;226:723–30.
[19] Hall F, Patel K, Stewart M. Interlacing results on matrices associated with graphs. J Combin Math Combin Comput 2009;68:113–27.
[20] Shi D, Chen G, Thong WW, Yan X. Searching for optimal network topology with best possible synchronizability. IEEE Circuits Syst Mag 2013;13(1):66–75.
[21] Chen G. Searching for best network topologies with optimal synchronizability: A brief review. IEEE/CAA J Autom Sin 2022;9(4):573–7.
[22] Newman ME. Modularity and community structure in networks. PNAS 2006;103(23):8577–82.
[23] Von Luxburg U. A tutorial on spectral clustering. Stat Comput 2007;17:395–416.
[24] Pothen A, Simon HD, Liou KP. Partitioning sparse matrices with eigenvectors of graphs. SIAM J Matrix Anal Appl 1990;11(3):430–52.
[25] Horn RA, Johnson CR. Matrix analysis. Cambridge: Cambridge University Press; 2012.
[26] Newman ME, Zhang X, Nadakuditi RR. Spectra of random networks with arbitrary degrees. Phys Rev E 2019;99(4):042309.
[27] Lu JA, Liu H, Chen J. Synchronization in complex dynamical networks. Beijing: Higher Education Press; 2016.
[28] Jeffreys H, Jeffreys B. Methods of mathematical physics. Cambridge: Cambridge University Press; 1999.
[29] Guo HM, Franz M. Topological insulator on the kagome lattice. Phys Rev B 2009;80(11):113102.
[30] Liu Z, Tao S, Liu H, Ma C, Li P, Cai Z, et al. Realization of material with an atomic ruby lattice. Nano Lett 2024;24(35):11075–81.
[31] Li D, Zhao Y, Deng Y, Wang Y. Rumor propagation in the framework of evolutionary game analysis. Chaos 2025;35(3).
[32] Cheng Y, Huo LA, Zhao L. Stability analysis and optimal control of rumor spreading model under media coverage considering time delay and pulse vaccination. Chaos Solitons Fractals 2022;157:111931.
[33] Siebert BA, Hall CL, Gleeson JP, Asllani M. Role of modularity in self-organization dynamics in biological networks. Phys Rev E 2020;102(5):052306.
[34] Križmančić M, Bogdan S. Adaptive connectivity control in networked multi-agent systems: A distributed approach. PLoS One 2024;19(12):e0314642.